Cyclotron Resonance of Electrons and Holes in Silicon and Germanium Crystals

G. DRESSELHAUS, A. F. KIP, AND C. KITTEL
Department of Physics, University of California, Berkeley, California

(Received December 16, 1954)

An experimental and theoretical discussion is given of the results of cyclotron resonance experiments on charge carriers in silicon and germanium single crystals near 4°K. A description is given of the light-modulation technique which gives good signal-to-noise ratios. Experiments with circularly polarized microwave radiation are described. A complete study of anisotropy effects is reported. The electron energy surfaces in germanium near the band edge are prolate spheroids oriented along ⟨111⟩ axes with longitudinal mass parameter $m_l=(1.58\pm0.04)m$ and transverse mass parameter $m_t=(0.082\pm0.001)m$. The electron energy surfaces in silicon are prolate spheroids oriented along ⟨100⟩ axes with $m_l=(0.97\pm0.02)m$; $m_t=(0.19\pm0.01)m$. The energy surfaces for holes in both germanium and silicon have the form

$$E(k)=Ak^2\pm[B^2k^4+C^2(k_x^2k_y^2+k_y^2k_z^2+k_z^2k_x^2)]^{\frac{1}{2}}.$$

We find, for germanium, $A=-(13.0\pm0.2)(\hbar^2/2m)$, $|B|=(8.9\pm0.1)(\hbar^2/2m)$, $|C|=(10.3\pm0.2)(\hbar^2/2m)$; and for silicon, $A=-(4.1\pm0.2)(\hbar^2/2m)$, $|B|=(1.6\pm0.2)(\hbar^2/2m)$, $|C|=(3.3\pm0.5)(\hbar^2/2m)$. A discussion of possible systematic errors in these constants is given in the paper.

1. INTRODUCTION

IN cyclotron resonance the current carriers in a solid are accelerated in spiral orbits about the axis of a static magnetic field H. The angular rotation frequency is

$$\omega_c=\pm eH/m^*c, \tag{1}$$

where m^* is the effective mass of the carrier. The experiment determines the effective mass directly, and is the first experiment to do so. Resonant absorption of energy from an rf electric field perpendicular to the static magnetic field occurs when the frequency of the rf field is equal to the cyclotron frequency $f_c=\omega_c/2\pi$. The motion is not unlike that of the particles in a cyclotron or simple magnetron. The $\pm$ choice in Eq. (1) indicates that holes and electrons will rotate in opposite senses in the magnetic field.

We consider the order of magnitude of several physical quantities relevant to the experiment. We make the estimates using $m^*/m\cong0.1$, which is not unrepresentative. For $f_c=24\,000$ Mc/sec, or $\omega_c=1.5\times10^{11}$ radians/sec, we have $H\cong860$ oersteds. The radius of the orbit is $r=v/\omega_c$. The mean radius for carriers in a Maxwellian velocity distribution at temperature T is

$$\bar{r}=\left(\frac{8kT}{\pi m^*}\right)^{\frac{1}{2}}\frac{1}{\omega_c}, \tag{2}$$

as $\bar{v}=(8kT/\pi m^*)^{\frac{1}{2}}$. For $T=4$°K, $\bar{v}\cong4\times10^6$ cm/sec, and $\bar{r}\cong3\times10^{-5}$ cm. The transition probability in cyclotron resonance is proportional to the square of the electric dipole moment; in electron spin resonance the transition probability is proportional to the square of the magnetic moment. As the maximum electric field in a resonant cavity is of the same order of magnitude as the maximum magnetic field, the ratio of the transition probabilities for cyclotron and for spin resonance will be of the order of

$$P_c/P_s\approx(e\bar{r})^2/\mu_B^2\approx10^{12} \tag{3}$$

for equal line widths, frequencies, and numbers of effective carriers. The Boltzmann factor in spin resonance is to be taken into account in the definition of an effective carrier. The substantial advantage favoring the detection of cyclotron resonance is partly lost because of the low carrier concentrations used in cyclotron resonance.

The line width is determined by the collision relaxation time τ, which describes the effect of collisions of the carriers with lattice vibrations, impurity atoms, and other imperfections. It is necessary that $\omega_c\tau\gtrsim1$ in order to obtain a distinctive resonance. In other words, the mean free path must be large enough so that the average carrier will get $1/2\pi$ of the way around a circle between successive collisions. For $\omega_c=1.5\times10^{11}$ sec^{-1}, we require $\tau\approx10^{-11}$ sec or longer. At room temperature the relaxation times of carriers in semiconductors and metals are commonly of the order of 10^{-13} to 10^{-15} second. It is usually necessary to work with high-purity crystals in the liquid hydrogen or liquid helium temperature range in order to obtain relaxation times which are long enough to permit the observation of cyclotron resonance with X- or K-band microwave equipment.

The theory of cyclotron resonance absorption is elementary, and for free particles goes back to Drude, Voigt, and Lorentz. Cyclotron resonance of free electrons in the earth's magnetic field has been observed in the propagation of radio waves in the ionosphere. The idea that it might be possible to carry out cyclotron resonance experiments in solids has been considered independently by a number of workers. In 1951 Dorfmann[1] published the suggestion of the possible application of cyclotron resonance to solids. Independently and simultaneously, Dingle[2] published his work on the

[1] J. Dorfmann, Doklady Acad. Sci. (U.S.S.R.) **81**, 765 (1951).
[2] R. B. Dingle, Ph.D. thesis, Cambridge University, 1951 (unpublished); Proceedings of the International Conference on Very Low Temperatures, edited by R. Bowers (Oxford, England, August 1951), p. 165; Proc. Roy. Soc. (London) **A212**, 38 (1952).

quantum theory of cyclotron resonance of a free particle, and also discussed the possible application to solids. Shockley[3] gave the solution of the problem of the cyclotron frequency for an ellipsoidal energy surface; his result is applicable directly to the conduction bands of silicon and germanium. He also derived expressions for the effective mobility in transverse and longitudinal cyclotron resonance. Later, Suhl and Pearson[4] reported an unsuccessful experimental attempt to detect cyclotron resonance in germanium at 77°K. The present authors[5] reported the first successful cyclotron resonance experiments, on germanium at 4°K. Our original results on germanium were incomplete, and important further developments for germanium have been reported by Lax, Zeiger, Dexter, and Rosenblum,[6] and by Dexter, Zeiger, and Lax.[7] The first work on silicon was reported concurrently by the Lincoln and Berkeley groups.

2. CLASSICAL THEORY OF CYCLOTRON RESONANCE FOR AN ISOTROPIC EFFECTIVE MASS

We give now a brief classical discussion of cyclotron resonance absorption by a carrier of isotropic effective mass. The theory will be generalized in later sections following a discussion of the experimental results. We review briefly the elementary classical theory of the process, assuming an isotropic effective mass m^* and an isotropic relaxation time τ, both independent of the velocity. In unpublished work we have developed the theory from the viewpoint of the Boltzmann transport equation,[8] but it is not worth while to reproduce the calculations here. The machinery of the Boltzmann equation is useful if one wishes to include a specific velocity dependence of the relaxation time, but we have no direct knowledge of the velocity dependence of the relaxation time in the circumstances of our experiments.

The equation of motion for the drift velocity is

$$m^*\left(\frac{d\mathbf{v}}{dt}+\frac{1}{\tau}\mathbf{v}\right)=e\left(\mathbf{E}+\frac{\mathbf{v}\times\mathbf{H}}{c}\right). \tag{4}$$

We take H as the static field along the z-axis and neglect the rf magnetic field. For plane-polarized radiation E_x, we have

$$m^*\left(i\omega+\frac{1}{\tau}\right)v_x=eE_x+\frac{e}{c}v_yH; \tag{5}$$

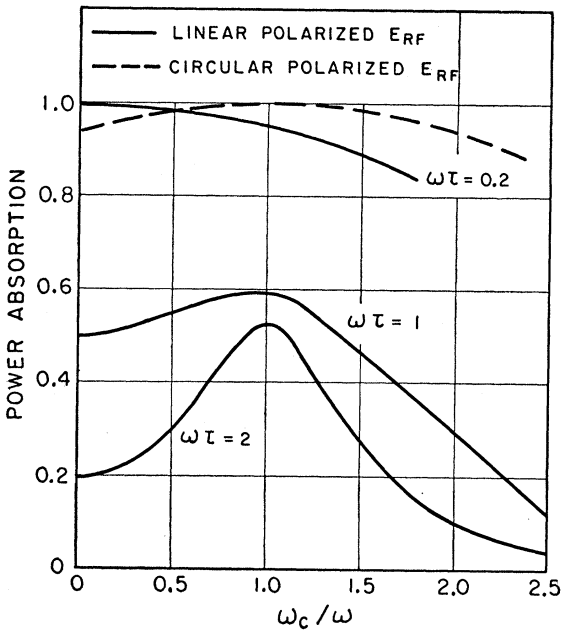

FIG. 1. Theoretical curves showing relative power absorption at constant frequency as a function of the static magnetic field intensity in units ω_c/ω, for various relaxation times in units $\omega\tau$. Curves are given for both linear polarization (Eq. [8]) and circular polarization of the rf field.

$$m^*\left(i\omega+\frac{1}{\tau}\right)v_y=-\frac{e}{c}v_xH.$$

We solve for v_x, finding for the complex conductivity,

$$\sigma=j_x/E_x=Nev_x/E_x=\sigma_0\left[\frac{1+i\omega\tau}{1+(\omega_c^2-\omega^2)\tau^2+2i\omega\tau}\right], \tag{6}$$

where

$$\sigma_0=Ne^2\tau/m^* \tag{7}$$

is the static conductivity; N is the carrier concentration. The losses are proportional to the real part of the conductivity. We express the result in convenient dimensionless form by writing $\nu=\omega\tau$, $\nu_c=\omega_c\tau$; the real part σ_R of σ is given by

$$\sigma_R/\sigma_0=\frac{1+\nu^2+\nu_c^2}{(1+\nu_c^2-\nu^2)^2+4\nu^2}. \tag{8}$$

This function is plotted in Fig. 1 for $\nu=0.2$, 1, and 2; it is seen that the resonance is quite well defined for $\nu=2$.

It is interesting to state in terms of the mobility the condition $\omega\tau>1$ for the observation of cyclotron resonance. In esu, $\tau=m^*\mu/e$; to have $\omega\tau>1$ requires $\mu>e/\omega m^*$. For $f=24\,000$ Mc/sec, the condition on μ expressed in practical units is, approximately,

$$(m^*/m)\mu>11\,000\ \text{cm}^2/\text{volt-sec}. \tag{9}$$

A high mobility does not in itself assure that a cyclotron resonance experiment is feasible; an appropriate average effective mass must also be considered. For narrow

[3] W. Shockley, Phys. Rev. **90**, 491 (1953).
[4] H. Suhl and G. L. Pearson, Phys. Rev. **92**, 858 (1953).
[5] Dresselhaus, Kip, and Kittel, Phys. Rev. **92**, 827 (1953).
[6] Lax, Zeiger, Dexter, and Rosenblum, Phys. Rev. **93**, 1418 (1954).
[7] Dexter, Zeiger, and Lax, Phys. Rev. **95**, 557 (1954).
[8] See, for example, the related calculation by R. Jancel and T. Kahan, J. phys. et radium **14**, 533 (1953); L. G. H. Huxley, Proc. Phys. Soc. (London) **B64**, 844 (1951).

energy gaps, the mobility divided by the gap energy may be a useful guide to relative relaxation times, as under some conditions $m^* \propto E_g$, approximately.

Several limiting situations are of interest:

(a) $\nu_c \gg \nu$; $\nu_c \gg 1$. This situation is found in very strong magnetic fields. We have

$$\sigma_R = \sigma_0/\nu_c^2 \propto 1/H^2, \tag{10}$$

so the losses well above the resonance field fall off as $1/H^2$. The carrier orbits are tightly coiled and very little drift is permitted in the direction of the electric field.

(b) $1 \gg \nu_c \gg \nu$. This situation is found at low frequencies at room temperature, or at low frequencies in weak magnetic fields at low temperatures. We have

$$\sigma_R/\sigma_0 \cong 1-\nu_c^2, \tag{11}$$

corresponding to a fractional resistivity change

$$\Delta\rho/\rho \cong \nu_c^2 = (\omega_c\tau)^2 = (\mu H/c)^2, \tag{12}$$

where the mobility is written as

$$\mu = e\tau/m^*. \tag{13}$$

This limit represents the low-frequency transverse magnetoresistance in the absence of a Hall electric field; in many actual problems, part of the transverse magnetoresistance is canceled[9] by the effect of the Hall field.

(c) $\nu \gg 1$; $\nu_c = 0$. This situation occurs in the infrared:

$$\sigma_R/\sigma_0 \cong 1/\nu^2. \tag{14}$$

(d) $\nu = \nu_c \gg 1$. This is the condition for cyclotron resonance. We have, from Eq. (8),

$$\sigma_R/\sigma_0 = 1/2. \tag{15}$$

Thus, at cyclotron resonance, the conductivity is one-half of the dc conductivity. If we had taken circularly polarized radiation in place of plane-polarized radiation, the ratio would have been unity. The factor one-half represents the selective absorption of one of the two circular components of a plane wave; the other component passes freely in the limit considered. The component which is absorbed at cyclotron resonance remains in phase with the drift velocity throughout the motion, just as in ordinary dc conductivity; hence the absorption of this component is identical with the dc absorption.

The rf conductivity at resonance is related to the rf conductivity at zero magnetic field by the ratio

$$\sigma_R(\text{res})/\sigma_R(H=0) = \nu_c^2/2, \tag{16}$$

provided $\nu_c \gg 1$. For $\omega_c\tau \approx 10$, the ratio $\sigma_R(\text{res})/\sigma_R(H=0)$ is of the order of 50.

We now consider the Q of the sample at cyclotron resonance. We suppose the specimen is located in the microwave cavity at a position of negligible rf magnetic field. The stored energy density is $\epsilon\langle E^2\rangle_{\text{Av}}/8\pi$; the energy dissipated per radian at resonance is $\sigma_R\langle E^2\rangle_{\text{Av}}/\omega$, so

$$Q_{\text{cycl}} = \epsilon\omega/8\pi\sigma_R = m^*\epsilon\omega/4\pi Ne^2\tau. \tag{17}$$

For the standard example described in the introduction,

$$Q_{\text{cycl}} \approx 10^{12}/N. \tag{18}$$

This may be compared with the estimated Q for electron spin resonance[10]:

$$Q_{\text{spin}} = (kT/N\mu_B^2)(\Delta\omega/\omega). \tag{19}$$

For the sake of comparison, we set the spin resonance line width equal to the cyclotron resonance line width. We take $\Delta\omega = 1/\tau$, so

$$Q_{\text{spin}} \cong kT/N\mu_B^2\omega\tau \approx 10^{24}/N \tag{20}$$

under the previous conditions. The requirement that a resonance may be detected may be stated roughly that for a given line width a certain threshold $1/Q$ must be exceeded, $1/Q$ being the measure of the absorption. It appears therefore that cyclotron resonance should be detectable at carrier concentrations lower by a factor of the order of 10^{12} than spin resonance; the factor arises principally from the relevant matrix elements, as we saw earlier in Eq. (3). There are several practical considerations which act to reduce the factor, but it would appear that it is in principle within the range of existing equipment to detect 10^4 carriers in cyclotron resonance.

The half-width at half σ_R on the σ_R *vs* ω curve is determined by the condition

$$\tau\Delta\omega = 1. \tag{21}$$

For broad lines the position of maximum absorption shifts slightly toward higher H. For $\omega\tau = 1$ the fractional shift is approximately 1/9; for $\omega\tau \gg 1$ the fractional shift is of the order of $1/8(\omega\tau)^2$, which will usually be unimportant. In our experiments on germanium and silicon at 4°K and 24 000 Mc/sec, the value of $\omega\tau$ was about 10.

Depolarization Effects

We show now that the electrostatic self-interaction of the resonance polarization may be neglected at the lower carrier concentrations with which we are concerned, although at higher concentrations new and undesirable effects enter. We consider the depolarizing fields associated with the shape of the sample; the effect of possible Lorentz fields is neglected. We suppose for simplicity that the sample has axial symmetry about the axis of the static magnetic field. In the axial plane the internal electric field is

$$E_i = E - LP, \tag{22}$$

where L is the depolarizing factor. The polarization P

[9] A. H. Wilson, *Theory of Metals* (Cambridge University Press, London, 1953), second edition p. 215.

[10] C. Kittel and J. M. Luttinger, Phys. Rev. **73**, 162 (1948).

is given by

$$P=\chi_0 E_i+Ne\int v dt=\chi_0 E_i-iNev/\omega; \quad (23)$$

here $\chi_0=(\epsilon-1)/4\pi$, and ϵ is the dielectric constant of the host crystal exclusive of carriers. The internal field is

$$E_i=\frac{E+i(LNev/\omega)}{1+L\chi_0}, \quad (24)$$

and the equation of motion becomes ($L_i=L/(1+L\chi_0)$).

$$m^*\left[i\left(\omega-\frac{L_iNe^2}{m^*\omega}\right)+\frac{1}{\tau}\right]\mathbf{v}=\frac{e}{1+L\chi_0}\mathbf{E}+(e/c)\mathbf{v}\times\mathbf{H}. \quad (25)$$

The effect of the carrier polarization is to replace ω in the equation for $\mathbf{v}$ by $\omega[1-(\omega_p/\omega)^2]$, where the plasma frequency ω_p is given by

$$\omega_p=(L_iNe^2/m^*)^{\frac{1}{2}}=(L_i\sigma_0/\tau)^{\frac{1}{2}}. \quad (26)$$

The effect will be important when ω_p is of the order of ω or larger. A critical concentration N_p may be defined by the relation

$$N_p=m^*\omega^2/L_ie^2. \quad (27)$$

In the standard example $N_p\cong 4\times 10^{12}/L$ cm^{-3}. For a sphere $L=4\pi/3$, so $N_p\cong 10^{12}$ cm^{-3}; for a flat disk one could quite easily get N_p up to 10^{14} cm^{-3}. In germanium with 10^{14} impurity atoms/cm^3 it appears that depolarization effects will enter somewhat above 10°K. It is very important to avoid depolarization effects, and this may be done by the use of thin specimens at low concentrations, with the rf electric field parallel to the plane of the specimen and the static magnetic field normal to the plane.

Depolarization effects can produce a fictitious cyclotron resonance in a limited temperature range in the following way: If $\omega\tau$ is too small for the normal cyclotron resonance to be observable, it may still be possible to have $\omega_p^2\tau/\omega\gtrsim 1$, so that a magnetoplasma resonance will appear at a field H such that

$$\omega\omega_c=\omega^2-\omega_p^2, \quad (28)$$

where ω_c is the cyclotron angular frequency. This equation describes the Zeeman effect of an oscillator with the natural frequency ω_p. If ω^2 may be neglected, we have the resonance condition

$$-\omega\omega_c\cong\omega_p^2=L_i\sigma_0/\tau=L_iNe^2/m^*. \quad (29)$$

We have observed in p-Ge near 20°K a resonance which possibly may arise from this effect; unlike the actual cyclotron resonances, the resonance field varied strongly with temperature and also with the shape of the specimen. A displacement of the cyclotron resonances in silicon has also been observed under conditions of higher carrier concentrations. A distinctive magnetoplasma resonance line has been observed in n-InSb; the line showed the expected dependence on frequency and on sample shape.

The magnetoplasma effect[11] appears to impose an upper limit to the carrier concentrations at which cyclotron resonance may be observed. It is hoped that the effect will be investigated further in order to establish whether or not the predicted limitation actually occurs. A background of nonresonant carriers is not necessarily troublesome, so it may be possible, for example, to detect cyclotron resonance of a subcritical concentration of electrons in the presence of a supercritical concentration of holes. A further apparent difficulty which may enter at the high carrier concentrations encountered in metals is that the diameter of the cyclotron orbit may be large in comparison with the skin depth. Unfortunately the relevant transport problem has not yet been solved, so one does not know to what extent the line shape and intensity depend on the ratio of orbit diameter to skin depth. In superconductors one has the plasma effect, and also the difficulty in obtaining penetration of the static magnetic field. Even if a superconducting film is used which is thin in comparison with the penetration depth for parallel static magnetic fields, it is not possible[12] for a field *normal* to the surface to penetrate uniformly over a useful area. A preliminary attempt in this laboratory by G. Feher to detect cyclotron resonance in a thin superconducting film was not successful; the negative result is not surprising, in view of the foregoing objections.

3. EXPERIMENTAL METHODS

A brief account will be given of the microwave apparatus which has been used in these experiments. The experimental techniques will be described, including the various methods which have been used to ionize electrons and holes. Sample preparation and mounting arrangements will be discussed. Some experiments which allowed discrimination between resonance absorption due to electrons and holes will be described.

Apparatus

In order to fulfill the requirement that $\omega_c\tau\geq 1$, the experiments have been performed at microwave frequencies, at or near 4°K, in the range of 9000 and 24 000 Mc/sec. The apparatus used is essentially the same as for conventional paramagnetic resonance experiments, except that the geometry is modified so that the microwave electric field is perpendicular to the external applied magnetic field. This is in contrast to the paramagnetic arrangement which puts the micro-

[11] C. Kittel, Proceedings of the 10th Solvay Congress, 1954 (unpublished).

[12] We consider the maximum radius R which a thin superconducting disk of thickness $a\ll$penetration depth d may have without significant perturbation of the normal field H_0. By the London equation $\mathbf{j}=\mathbf{r}\times\mathbf{H}_0/2\Lambda c$, this current produces in turn a magnetic field $\Delta H=(2\pi a/c)\int(j/r)dr=(2\pi\Lambda c^2)aRH_0$. We will have $(\Delta H/H_0)\ll 1$ if $aR\ll 2d^2$, using the relation $d^2=\Lambda c^2/4\pi$. This effect was suggested by G. Feher.

wave magnetic field perpendicular to the external magnetic field. Absorption of energy under cyclotron resonance conditions has been determined by measuring the change in the Q of a microwave cavity in which the sample has been placed. The applied magnetic field may be varied in order to obtain the spectrum of power absorption in the sample *vs* the magnetic field. From the absorption spectrum the effective masses may be obtained directly from the equations derived in Secs. 4 and 5 below.

The microwave circuit is a conventional one. Microwave power from a stabilized klystron is fed into the test cavity through a magic tee; 2K39 and 2K33 klystrons have been used at the lower and higher frequencies, respectively. Some of the power reflected back from the test cavity reaches a crystal detector in another arm of the tee. The fourth arm of the tee is fitted with a matched load so that all power incident on the crystal has been reflected from the cavity. A change in the loaded Q of the cavity resulting from cyclotron absorption in the sample causes a change in the power reflected to the crystal. This change in reflected power is proportional to the loss in the sample for small signals (i.e., for sample losses small compared to other losses in the cavity). For small signals, the change in output voltage of the crystal will be proportional to the change in power incident upon it. Thus, the crystal gives a voltage signal which measures the variation of power absorbed by the sample as the magnetic field is varied.

One of the several modulation techniques is used to produce an ac signal at the crystal. The ac signal is passed through a detection channel consisting of an amplifier and a lock-in detector, the output of which is put on a pen recorder. A 1000-cps modulation frequency is used. The external magnetic field is caused to sweep slowly from zero to a maximum of 10 000 oersteds by means of an electronic control on the field coil of a motor generator used to provide the magnet current. Field markers are applied periodically to the pen recorder. These markers are obtained from a rotating coil in the magnetic field. The signal from this coil is balanced on a potentiometer against another signal from a coil mounted on the same shaft which rotates in the field of a fixed permanent magnet. The value of any given field is determined by the potentiometer setting which gives a null signal.

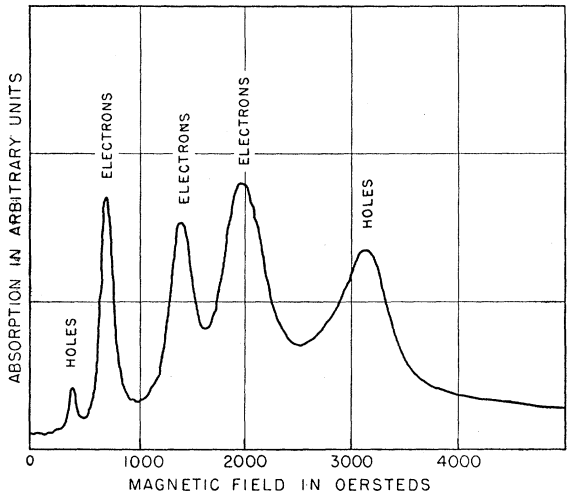

FIG. 2. Typical cyclotron resonance results in germanium near 24 000 Mc/sec and 4°K: direct copy from a recorder trace of power absorption *vs* static magnetic field in an orientation in a (110) plane at 60° from a [100] axis.

In all the experiments low temperatures are provided by liquid helium. In most experiments liquid helium is allowed to enter the cavity, so that the sample is immersed in helium. In some experiments pumping on the helium has allowed reduction of the temperature to 2°K.

In experiments with plane-polarized microwaves the samples were placed inside rectangular cavities made from wave guide stock. The cavity was coupled to the wave guide through an iris containing an appropriate coupling hole. The construction of cavities used in the circularly polarized microwave experiments will be discussed below under that heading.

Experimental Technique

At the low temperatures required in these experiments, the equilibrium number of free charge carriers is usually too small to allow observation of resonance absorption. In the original experiments on germanium it was found that in both frequency ranges used the microwave electric field in the cavity was sufficient to cause ionization of impurity atoms by multiplication processes taking place in the sample. Only electrons or only holes appear to be produced by this ionization process, depending on whether n- or p-type germanium is used. This results from the fact that energies given to the carriers by the microwave field are only enough to cause ionization of impurity atoms ($\sim$0.01 ev in germanium), and not enough to produce electron-hole pairs by the removal of electrons from the valence band to the conduction band (0.7 ev in germanium). In silicon, where the ionization energy of the impurity atoms is $\sim$0.05 ev, the available microwave power is insufficient to produce ionization, and other methods must therefore be used to produce free charge carriers. In experiments using the microwave ionization technique, the microwave power was amplitude-modulated in order to provide an ac signal for the detection channel.

The microwave ionization method provides fairly satisfactory information on the positions of peaks in the absorption curve. However, the observed widths of the resonance lines may vary between wide limits, depending on the microwave power level used. This effect results from the dependence of the multiplication process on the applied magnetic field. Thus, near a resonance peak, charge carriers pick up more energy from the microwave electric field and hence cause more

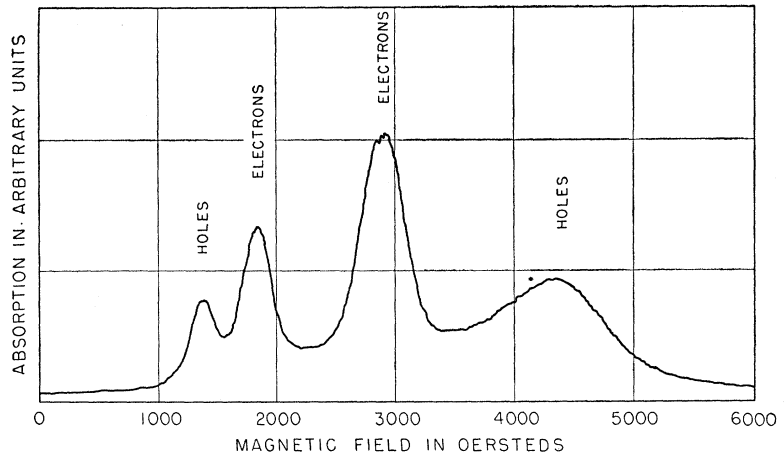

FIG. 3. Typical cyclotron resonance results in silicon near 24 000 Mc/sec and 4°K: static magnetic field orientation in a (110) plane at 30° from a [100] axis.

multiplication. Since the size of the absorption peak will vary with the number of carriers present, peak heights can be enormously increased, resulting in apparently very narrow lines. Lines as narrow as 10 oersteds have been observed in some cases where microwave power levels were so low that effective multiplication occurred only very close to the resonance peak.

A more satisfactory method of producing free charge carriers involves the use of light excitation; it was first used by Dexter, Zeiger, and Lax.[13] In this technique, light from an incandescent source is focused on the sample through a hole in the cavity. Since the light produces hole-electron pairs, both hole and electron resonance is observed, regardless of whether the sample is *n*- or *p*-type. The first observations on silicon were made by this technique.[14] In our first experiments using light excitation, amplitude modulation of the microwaves was used to provide an ac signal.

A slight modification of the optical excitation method is the most satisfactory method so far used.[15] The modification consists in modulating the light beam by means of a rotating disk. This results in a modulation of the free carrier density, which in turn gives a modulated microwave absorption signal for operation of the detection channel. An auxiliary light source incident on a photocell is modulated by the same rotating disk. After amplification the signal from the photocell is used as the reference signal for the lock-in detector. The light-modulation method gives a very large improvement in signal-to-noise ratio over the earlier techniques. Figures 2 and 3 show typical recorder tracings of resonance lines in germanium and silicon crystals.

Because of the high dielectric constants of both silicon and germanium, samples placed in a cavity seriously perturb the resonant frequency of the cavity. Furthermore, since at all but very low temperatures the samples are very lossy because of their high conductivity, it is difficult to determine the resonant frequency without cooling to liquid-helium temperature. Both problems are minimized by using small samples. A typical sample is a disk about 3 mm in diameter and about 0.5 mm thick. Samples have usually been prepared by rough-cutting from a single crystal, grinding to size with abrasives, and etching the surface for several minutes in an etch made up of 1 cc HF, 1 cc H_2O_2 (30 percent), and 4 cc H_2O.

The importance of anisotropy in the effective masses of silicon and germanium requires that data be obtained as a function of crystal orientation. A sample cut with its surface in the (110) plane, oriented so that the applied field can be directed along the [001], [1$\bar{1}$0], and [1$\bar{1}$1] directions by rotation of the sample, provides all of the necessary anisotropy information. To allow this rotation while the cavity is immersed in liquid helium, the sample is fastened with coil dope to a mushroom-shaped Lucite holder. This holder is put inside the cavity, with its stem inserted through a small hole in the broad face of the cavity into a hole in the middle of a brass wheel outside the cavity. The wheel can be rotated from outside the Dewar in 1° steps. The light beam shines on the sample through another hole in the opposite side of the cavity. The samples were oriented by x-ray diffraction measurements by Professor J. Washburn. The effective mass data are presented in Secs. 4 and 5 below.

In the original experiments on germanium it was of interest to verify the sign of the charge carriers involved. For this reason, experiments using circularly polarized microwaves were carried out, using *n*- and *p*-type samples in both frequency ranges. Absorption was observed only when the direction of circular polarization corresponded to the direction of rotation of the charge carriers.

[13] Dexter, Zeiger, and Lax, Phys. Rev. **95**, 557 (1954).
[14] Dexter, Lax, Kip, and Dresselhaus, Phys. Rev. **96**, 222 (1954).
[15] A. F. Kip, Physica **20**, 813 (1954).

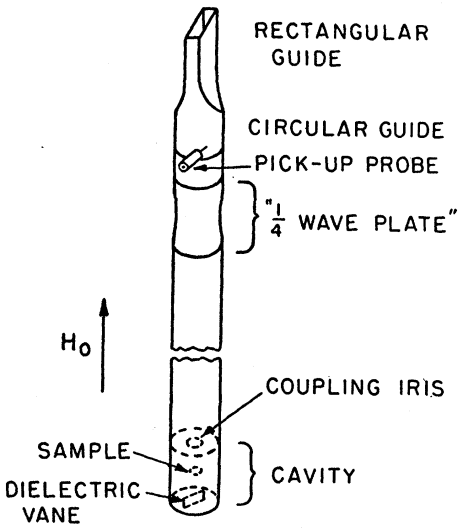

FIG. 4. Experimental arrangement for circular polarization studies of cyclotron resonance.

A description will be given of the problems involved in the production and use of circularly polarized microwaves. The klystron power was taken from a conventional rectangular guide through a gradual transition into circular guide, as shown in Fig. 4. The microwaves then passed through a microwave quarter-wave plate into another guide of circular cross section, and thence through a circular iris into a cylindrical cavity. The quarter-wave plate consisted simply of a section of several wavelengths of circular guide which had been squeezed into an appropriate elliptical shape. If the polarized microwaves from the rectangular guide are passed into this elliptical section with the plane of polarization at 45° to the axes of the ellipse, two mutually perpendicular modes of equal intensity will be transmitted through the section. Since the wave velocity depends on the transverse guide dimension perpendicular to the E vector, these two modes will travel with different velocities. Adjustment of ellipticity and length of the elliptical section produces a quarter wavelength shift in the phase of the two modes. This adjustment is made empirically by use of an analyzer placed at the position of the cavity at the end of the circular guide. The analyzer is constructed of a circular guide which makes a transition to a rectangular guide. A crystal detector is placed at the termination of the rectangular guide. Since the rectangular guide will transmit only a polarized wave, the analyzer will measure the intensity of the wave polarized in any given plane, depending on the analyzer orientation. When complete circular polarization is achieved, the power picked up by the crystal is independent of the orientation of the analyzer. In order to prevent reflection of power not accepted by the rectangular guide, both the analyzer and the transition from rectangular to circular guide are provided with absorbing fins placed in the circular guide. These fins are so oriented as to absorb all microwave components not transmitted or accepted by the rectangular guide.

Once circularly polarized waves are incident on the iris of the circular cavity, there remains only the problem of insuring that the cavity has perfect microwave cylindrical symmetry. Any departure from this symmetry will result in two different resonance frequencies for the two mutually perpendicular modes into which the circularly polarized mode can be analyzed. In general, satisfactory symmetry will not be automatically achieved; therefore, provision must be made for adjustment of symmetry. This is done in the following way: A small rectangular fin of polystyrene is placed in the end of the cylindrical cavity. The fin can be rotated about the axis of the cavity, and can be inserted a variable distance from the end wall of the cavity. The cylindrical axis passes through the plane of the fin. The plane of the fin is rotated until it contains the E vector of the plane-polarized component for which the wavelength in the cavity is longest. Because of its dielectric constant the polystyrene makes the cavity look longer to this mode without materially affecting the perpendicular mode. Once proper orientation is obtained, the fin is inserted further into the cavity where the E field is higher and hence the perturbation is greater. The adjustment is made empirically until the two perpendicular modes are completely degenerate. The method involves sweeping the klystron frequency and adjusting the fin until the two resonant modes of the cavity are made to coincide in frequency. After adjustment of the cavity, the small cylindrical sample is placed accurately on the axis of the cavity, so as to maintain the degeneracy of the two modes. The sample is held in position by partially filling the cavity with layers of tightly fitting Styrofoam, between which the sample is placed.

The problem of detection of the power reflected from the cylindrical cavity is very simple with the arrangement used. A pickup probe is placed in the cylindrical guide of the klystron side of the quarter-wave plate. This probe is oriented perpendicularly to the E vector of the wave coming from the klystron through the rectangular guide, and hence does not pick up a signal from this wave. However, after the wave travels through the quarter-wave plate into the cavity and is reflected back through the quarter-wave plate again, it has been rotated through 90° and hence is picked up by the probe. The probe leads to a crystal detector. Amplitude modulation of the microwave power allows the usual detection channel to be used on the output signal from the crystal.

The magnetic field must be perpendicular to the microwave E vector, and hence must be along the axis of the cylindrical cavity. We therefore used a solenoidal air core electromagnet into which the Dewars and cavity were inserted. The direction of circular polarization obtained was confirmed by observing electron

spin resonance in an organic free radical, this resonance occurring in the same sense as electron cyclotron resonance. Circular polarization has been used only on germanium, where microwave ionization is possible.

A third method of ionization has also been used which allows the selective observation of one sign of charge carrier, depending on whether n- or p-type materials are used. In this method voltage is applied to the sample through soldered contacts. The voltage is modulated at the standard 1000-cps rate to give the required ac signal for the detection channel. This method gives the same selective production of conduction electrons or holes as given by the microwave ionization method. It has the advantage of applicability to silicon, and gives much better signal-to-noise ratio. The resonance peaks observed are broader than for optically excited carriers, probably because of shorter relaxation times involved. Shorter relaxation times are probably the result of the higher carrier energies produced by the applied voltage. In this method the sample is placed just outside a small hole in the broad face of the rectangular cavity. This allows the sample to be seen by the microwaves and at the same time avoids the problems involved in bringing the wires carrying the voltage into the cavity.

4. THEORY OF CYCLOTRON RESONANCE IN THE CONDUCTION BAND OF GERMANIUM AND SILICON

The neighborhood of the conduction band edge in both germanium and silicon consists of a set of spheroidal energy surfaces located in equivalent positions in k-space. We discuss now the theory of cyclotron resonance for surfaces of this character. We choose Cartesian coordinate axes with the z-axis parallel to the figure axis of the spheroid, and we measure the wave vector components from the center of the spheroid. For points in k-space sufficiently close to a band edge point, the energy is described by the equation

$$E(\mathbf{k})=\hbar^2\left(\frac{k_x^2+k_y^2}{2m_t}+\frac{k_z^2}{2m_l}\right). \tag{30}$$

Here m_l is the longitudinal mass parameter and m_t is the transverse mass parameter. We have no evidence as to the range in k-space over which this expression is adequate; no departures were observed in our experiments.

We wish now to discuss the energy levels in the presence of a uniform static field H. The usual procedure is to take the effective Hamiltonian,

$$\mathcal{H}(\mathbf{P})=\frac{P_x^2+P_y^2}{2m_t}+\frac{P_z^2}{2m_l}, \tag{31}$$

and solve the equations of motion

$$\mathbf{v}=\nabla_P\mathcal{H}(\mathbf{P}); \tag{32}$$

$$d\mathbf{P}/dt=e[\mathbf{E}+(1/c)\mathbf{v}\times\mathbf{H}]. \tag{33}$$

Here $\mathbf{P}=\mathbf{p}-e\mathbf{A}/c$, where p is the momentum and $\mathbf{A}$ the vector potential.

This procedure in a restricted form was discussed by Jones and Zener[16]; recent discussions have been given by Shockley,[17] Luttinger,[18] and Adams.[19]

Shockley[20] has given the solution of the cyclotron frequency problem for a general ellipsoidal energy surface. We indicate the method of solution here. For the spheroidal surface (31),

$$\mathbf{v}=(P_x/m_t;\ P_y/m_t;\ P_z/m_l). \tag{34}$$

We take

$$\mathbf{H}=H(\sin\theta;\ 0;\ \cos\theta). \tag{35}$$

Then Eq. (33) becomes, letting $\omega_t=eH/m_tc$ and $\omega_l=eH/m_lc$,

$$\begin{aligned} i\omega P_x-\omega_t P_y\cos\theta&=0;\\ i\omega P_y-\omega_l P_z\sin\theta+\omega_t P_x\cos\theta&=0;\\ i\omega P_z+\omega_t P_y\sin\theta&=0. \end{aligned} \tag{36}$$

The associated secular equation has the solution

$$\omega^2=\omega_t^2\cos^2\theta+\omega_t\omega_l\sin^2\theta. \tag{37}$$

Thus, the effective mass determining the cyclotron frequency when the static magnetic field makes an angle θ with the longitudinal axis of the energy surface is

$$\left(\frac{1}{m^*}\right)^2=\frac{\cos^2\theta}{m_t^2}+\frac{\sin^2\theta}{m_tm_l}. \tag{38}$$

In Fig. 5 we give a plot of the experimental points obtained for electrons in germanium at 4°K as a function of the angle between the direction of the static magnetic field in a (110) plane and a [001] direction lying in the plane. The mass values derived from the theoretical fit to the experimental points are $m_l=(1.58\pm0.04)m$ and $m_t=(0.082\pm0.001)m$; we assume that there are a set of crystallographically equivalent energy spheroids oriented along the ⟨111⟩ directions in the Brillouin zone. Lax[21] *et al.* have reported $m_l=1.3m$ and $m_t=0.08m$ from a similar experiment. Our original observation[22] of one line in the [100] direction with $m^*=0.11m$ is in fair agreement with the later results.

In Fig. 6 we give a plot of the experimental points

[16] H. Jones and C. Zener, Proc. Roy. Soc. (London) **A144**, 101 (1934).
[17] W. Shockley, *Electrons and Holes in Semiconductors* (D. van Nostrand Company, New York, 1950), pp. 424 ff.
[18] J. M. Luttinger, Phys. Rev. **84**, 814 (1951); see also J. M. Luttinger and W. Kohn, Phys. Rev. **97**, 869 (1955).
[19] E. N. Adams, Phys. Rev. **85**, 41 (1952); **89**, 633 (1953).
[20] W. Shockley, Phys. Rev. **90**, 491 (1953); the problem had arisen also in connection with the de Haas-van Alphen effect.
[21] Lax, Zeiger, Dexter, and Rosenblum, Phys. Rev. **93**, 1418 (1954).
[22] See reference 4.

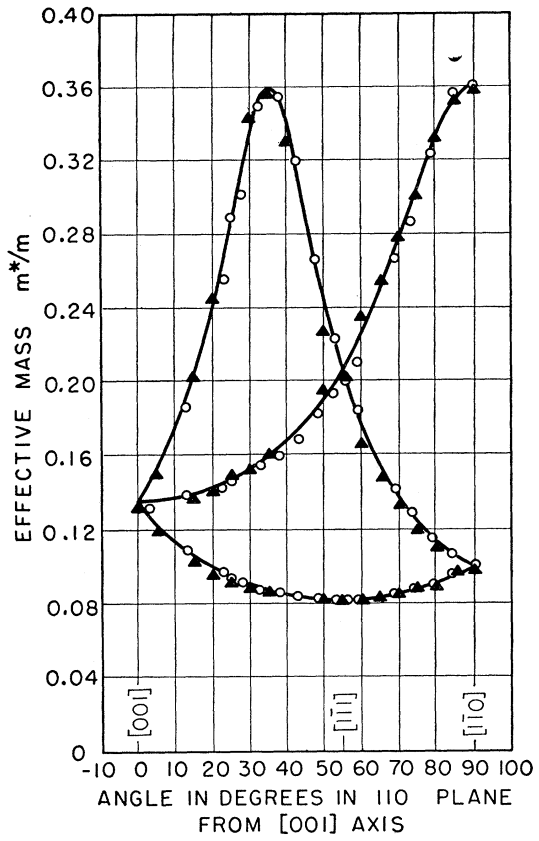

FIG. 5. Effective mass of electrons in germanium at 4°K for magnetic field directions in a (110) plane; the theoretical curves are calculated from Eq. (38), with $m_l=1.58m$; $m_t=0.082m$. The different types of points indicate different runs.

obtained for electrons in silicon at 4°K as a function of the angle between the direction of the static magnetic field in a (110) plane and a [001] direction lying in the plane. The theoretical curves are drawn for $m_l=(0.97\pm0.02)m$ and $m_t=(0.19\pm0.01)m$; we assume that there are a set of crystallographically equivalent energy spheroids oriented along the ⟨100⟩ directions in the Brillouin zone. In earlier work[23] the values $m_l=0.98m$ and $m_t=0.19m$ were reported under similar conditions.

Theoretical calculations of band structure have not reached as yet a state of development which permits the deductive derivation of the central features of the conduction band energy surfaces found experimentally. The most ambitious theoretical program has been that undertaken by F. Herman for germanium, but the band edge points turn out to be too sensitive to the details of the calculation to be reliable. Herman[24] has suggested, however, that the conduction band energy minima in silicon and germanium may arise from different bands: in silicon the band which at $k=0$ is a representation Γ_{15}^- of the cubic group is thought to lie lowest, whereas in germanium the lowest band at $k=0$ is thought to be a representation of Γ_2^- of the cubic group.

The structure of the conduction band edge of germanium determined by cyclotron resonance is consistent with the interpretation by Meiboom and Abeles[25] and by Shibuya[26] of magnetoresistance measurements on n-Ge by Estermann and Foner[27] and by Pearson and Suhl.[28] Similarly, the cyclotron resonance results for the conduction band edge of silicon are consistent with the magnetoresistance results of Pearson and Herring[29] on n-Si. In fact, the assignment of the energy surfaces in silicon to electrons or holes depends on the correlation with the magnetoresistance data.

In Sec. 3, it was found that in a circular polarization experiment on an n-Ge crystal in conditions of rf ionization with $H\|[100]$, absorption was observed only for one sense of the static magnetic field and not for the opposite sense. If the orbit of an electron is circular, absorption of circularly polarized radiation should occur only for one sense, but with an elliptical orbit there should be some absorption also in the opposite sense of the static field. We now calculate this absorption for a general orientation of the energy surface relative to the static magnetic field. The equations of motion are, using (33), (35), (36) and including an isotropic relaxation time τ,

$$(i\omega+1/\tau)P_x-\omega_t P_y=eE; \tag{39}$$

$$(i\omega+1/\tau)P_y+(\omega_0^2/\omega_t)P_x=-ieE. \tag{40}$$

The coordinate axes are chosen with the static magnetic field in the z-direction and the rf electric field in the xy plane; the energy surface is rewritten so that the principal axis of the surface makes an angle θ with the z-axis. The solution is independent of P_z, and we have set $P_z=0$ for convenience. If $\omega\tau\gg1$, the ratio $\mathfrak{R}$ of the power absorption at resonance in the weak sense of rotation to that in the strong sense of rotation is found to be

$$\mathfrak{R}=\left(\frac{m^*-m_t}{m^*+m_t}\right)^2. \tag{41}$$

For electrons in germanium with the static magnetic field in the [100] direction we have $\mathfrak{R}\cong0.06$, which is not inconsistent with the observations.

5. THEORY OF CYCLOTRON RESONANCE IN THE VALENCE BAND

The structures of the valence band edges of germanium and silicon are qualitatively similar. We discuss first the theory of the form of the energy surfaces near the band edge and secondly, the connection between

[23] Dexter, Lax, Kip, and Dresselhaus, Phys. Rev. **96**, 222 (1954).
[24] F. Herman, Phys. Rev. **95**, 847 (1954).
[25] S. Meiboom and B. Abeles, Phys. Rev. **95**, 31 (1954).
[26] M. Shibuya, Phys. Rev. **95**, 1385 (1954).
[27] I. Estermann and A. Foner, Phys. Rev. **79**, 365 (1950).
[28] G. L. Pearson and H. Suhl, Phys. Rev. **83**, 768 (1951).
[29] G. L. Pearson and C. Herring, Physica **20**, 975 (1954).

the cyclotron frequencies and the parameters which define the energy surfaces. The complete details of the calculations will be given in the doctoral thesis of G. Dresselhaus, of which a limited number of copies may be available for distribution by request late in 1955.

Everything we know at present indicates that the valence band edge occurs at the center of the Brillouin zone ($k=0$), at which point the band edge state has a threefold orbital degeneracy if the spin-orbit interaction is not considered. According to calculations by Herman[30] and others, it is most likely that the degenerate wave functions transform under the operations of the full cubic group according to the representation Γ_{25}^+ in the notation of Bouckaert, Smoluchowski, and Wigner,[31] or Γ_5^+ in the rotation of Von der Lage and Bethe.[32] In chemical language, the degenerate wave functions at the valence band edge have the transformation properties of p-orbitals arranged with opposite sign (bonding) on each of the two fcc lattices which compose the diamond structure. With spin-orbit interaction we have to deal at the valence band edge with bonding $p_{\frac{3}{2}}$ orbitals. The treatment below is quite general within the scope of the one-electron approximation; we do not make a tight binding assumption.

In order to establish a notation we first set up the solution to the problem without spin-orbit interaction, as has been discussed briefly by Shockley.[33] We will then extend the treatment to the actual problem with spin-orbit interaction. We make use of the pseudo-Bloch function representation introduced by Kittel and Mitchell.[34]

We make an arbitrary choice of a basis for the representation Γ_{25}^+ at $k=0$, taking the three degenerate states to transform as $\epsilon_1^+\sim yz$; $\epsilon_2^+\sim zx$; $\epsilon_3^+\sim xy$, following here, as below, the notation of Von der Lage and Bethe. We now construct three pseudo-Bloch functions from the original basis; that is, we construct by perturbation theory three functions $u_{\mathbf{k}}{}^i(\mathbf{r})e^{i\mathbf{k}\cdot\mathbf{r}}$ which are eigenfunctions of the crystal translation operator but which are not in general eigenfunctions to the first order in $\mathbf{k}$ of the Hamiltonian. However, linear combinations of the $u_{\mathbf{k}}{}^i$ diagonalize the Hamiltonian to the first order in $\mathbf{k}$. The perturbation term in the Hamiltonian is $\mathcal{H}'=\hbar\mathbf{k}\cdot\mathbf{p}/m$, where $\mathbf{p}=-i\hbar\nabla$ is the momentum operator. Thus,

$$u_{\mathbf{k}}{}^i(\mathbf{r})=\epsilon_i{}^+ + (\hbar/m)\mathbf{k}\cdot\sum_{l\alpha j}\frac{|l\alpha j\rangle\langle l\alpha j|\,\mathbf{p}\,|i+\rangle}{E_0-E_{l\alpha}}, \quad (42)$$

where $l\alpha j$ denotes the state j belonging to the representation α in the band l; E_l is the energy of the lth band at $\mathbf{k}=0$.

[30] F. Herman, Physica **20**, 801 (1954).
[31] Bouckaert, Smoluchowski, and Wigner, Phys. Rev. **50**, 58 (1936).
[32] F. C. Von der Lage and H. Bethe, Phys. Rev. **71**, 612 (1947).
[33] W. Shockley, Phys. Rev. **78**, 173 (1950).
[34] C. Kittel and A. H. Mitchell, Phys. Rev. **96**, 1488 (1954).

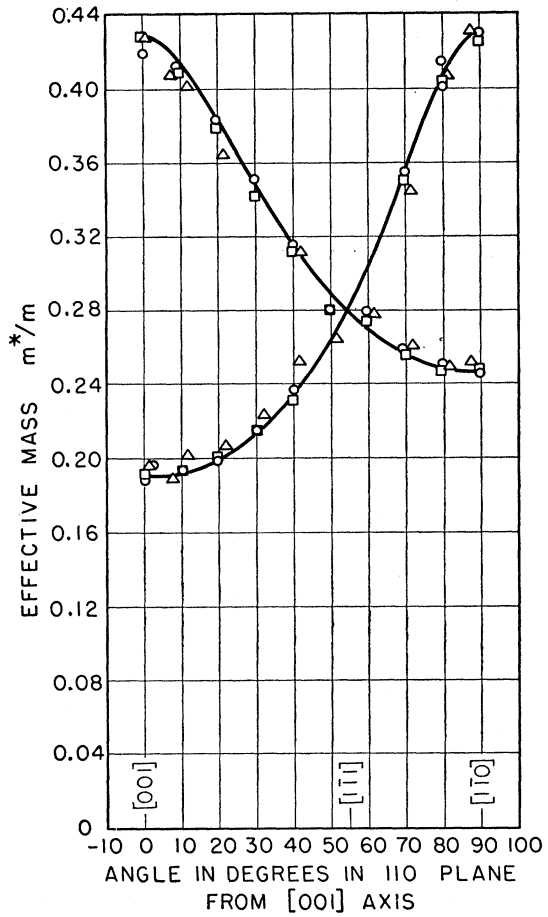

FIG. 6. Effective mass of electrons in silicon at 4°K for magnetic field directions in a (110) plane; the theoretical curves are calculated from Eq. (38), with $m_l=0.98m$; $m_t=0.19m$.

The perturbation matrix in this representation has the form

$$\langle r+|\mathcal{H}'|s+\rangle=\frac{\hbar^2}{m^2}\sum_{l\alpha j}\frac{\langle r+|\mathbf{k}\cdot\mathbf{p}|l\alpha j\rangle\langle l\alpha j|\mathbf{k}\cdot\mathbf{p}|s+\rangle}{E_0-E_{l\alpha}}, \quad (43)$$

as the matrix elements of $\mathbf{p}$ among the states $\epsilon_i{}^+$ are all zero. We can determine the dependence of $\langle r|\mathcal{H}'|s\rangle$ on the components of $\mathbf{k}$ by a simple observation. If all the $E_{l\alpha}$ were equal, say to E_1, the sum above could be carried out, giving

$$\langle r|\mathcal{H}'|s\rangle=\frac{\hbar^2}{m^2}\frac{\langle r|\mathcal{H}'^2|s\rangle}{E_0-E_1}. \quad (44)$$

We see immediately from the transformation properties of the $\epsilon_i{}^+$ that

$$\langle 1+|\mathcal{H}'^2|2+\rangle\propto k_xk_y, \quad (45)$$

with similar relations for other matrix elements. The form of each element as determined in this way will not change as we relax the above restriction on $E_{l\alpha}$.

The perturbation matrix is clearly of the form

$$\begin{vmatrix} Lk_x^2+M(k_y^2+k_z^2)-\lambda & Nk_xk_y & Nk_xk_z \\ Nk_xk_y & Lk_y^2+M(k_x^2+k_z^2)-\lambda & Nk_yk_z \\ Nk_xk_z & Nk_yk_z & Lk_z^2+M(k_x^2+k_y^2)-\lambda \end{vmatrix}=0. \tag{46}$$

Here

$$L=\frac{\hbar^2}{m^2}\sum_{l\alpha j}\frac{\langle 1+|p_x|l\alpha j\rangle\langle l\alpha j|p_x|1+\rangle}{E_0-E_{l\alpha}};$$

$$M=\frac{\hbar^2}{m^2}\sum_{l\alpha j}\frac{\langle 1+|p_y|l\alpha j\rangle\langle l\alpha j|p_y|1+\rangle}{E_0-E_{l\alpha}};$$

$$N=\frac{\hbar^2}{m^2}\sum_{l\alpha j}\frac{\langle 1+|p_x|l\alpha j\rangle\langle l\alpha j|p_y|2+\rangle+\langle 1+|p_y|l\alpha j\rangle\langle l\alpha j|p_x|2+\rangle}{E_0-E_{l\alpha}}. \tag{47}$$

The energy eigenvalue E_k is related to a root λ by

$$E_k=(\hbar^2/2m)k^2+\lambda. \tag{48}$$

We now examine in detail the matrix elements which occur in the sums L, M, and N above. We note first the selection rules on $\langle r+|\mathbf{p}|l\alpha j\rangle$; $\mathbf{p}$ is a vector and transforms as the representation Γ_{15}^-. The direct product

$$\Gamma_{25}^+\times\Gamma_{15}^-=\Gamma_{12}^-+\Gamma_{15}^-+\Gamma_2^-+\Gamma_{25}^-, \tag{49}$$

so that only the four representations on the right can perturb the valence band edge. The approximate order in energy of the several representations at $\mathbf{k}=0$ in germanium is shown in Fig. 7, based on calculations by F. Herman.[35] It is seen that the states Γ_2^-, Γ_{15}^-, and Γ_{12}^- in the conduction band are likely to provide the most effective perturbations on the state Γ_{25}^+ under consideration.

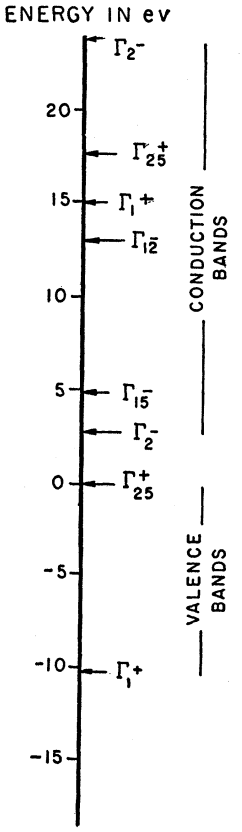

FIG. 7. Proposed order of the energy levels at $\mathbf{k}=0$ in germanium.

There are a number of relations which simplify the matrix elements. Although we do not intend to calculate the matrix elements, we will learn more from the energy surfaces as determined experimentally if we can simplify the expressions for the matrix elements. We first observe that the sum over representations α in L above need be carried out only over the representations Γ_2^- and Γ_{12}^-, as the other matrix elements are seen to vanish on examining the reflection properties of the integrands over the basal planes. For example, we know $\epsilon_1^+\sim yz$ and $p_x\sim x$, so $\epsilon_1^+p_x\sim xyz$. Reference to character tables shows that the characters of the representations Γ_{15}^-, Γ_{25}^- under reflections in the basal planes are positive, while xyz changes sign on reflection; therefore, the corresponding matrix elements vanish. We note the operation JC_4^2 is equivalent to a reflection. In a similar way we see the sum over representations α in M above need be carried out only over representations Γ_{15}^- and Γ_{25}^-.

We now show that L, M, N can be expressed in terms of a single matrix element for each representation, so the sums are reduced essentially to sums over the band index; in practice only one band is expected to contribute significantly. For the Γ_2^- representation, we define

$$F=\frac{\hbar^2}{m^2}\sum_l\frac{|\langle 1+|p_x|\beta_l^-\rangle|^2}{E_0-E_l}, \tag{50}$$

where β_l^- belongs to the one-dimensional representation Γ_2^-. For the Γ_{12}^- representation, we define

$$G=\frac{\hbar^2}{m^2}\sum_l\frac{|\langle 1+|p_x|\gamma_{1l}^-\rangle|^2}{E_0-E_l}. \tag{51}$$

[35] F. Herman (private communication); we are indebted to Dr. Herman for his cooperation on this and other occasions.

We choose γ_1, γ_2 so that the group elements are represented by unitary matrices; this is not done by Von der Lage and Bethe. For example, we take $\gamma_1=x^2+\omega y^2+\omega^2 z^2$ and $\gamma_2=x^2+\omega^2 y^2+\omega z^2$ as a pair of functions transforming according to Γ_{12}^+, where $\omega^3=1$. If we denote $\langle 1+|p_x|\gamma_1^-\rangle$ by R, we have

$$\langle 1+|p_x|\gamma_2^-\rangle=-R, \tag{52}$$

as is seen on rotation by $\pi/2$ about the x-axis. By similar considerations we may show that

$$\langle 2+|p_y|\gamma_1^-\rangle=-\omega^2\langle 2+|p_y|\gamma_2^-\rangle=\omega R. \tag{53}$$

Using (52), we have

$$L=F+2G. \tag{54}$$

For Γ_{15}^- representation, we define

$$H_1=\frac{\hbar^2}{m^2}\sum_l \frac{|\langle 1+|p_y|\delta_{3l}^-\rangle|^2}{E_0-E_l}, \tag{55}$$

where δ_3^- belongs to Γ_{15}^-. The matrix elements with δ_1^-, δ_2^- vanish, as seen by their behavior on reflection in the appropriate basal planes. For the Γ_{25}^- representation, we define

$$H_2=\frac{\hbar^2}{m^2}\sum_l \frac{|\langle 1+|p_y|\epsilon_{3l}^-\rangle|^2}{E_0-E_l}, \tag{56}$$

where ϵ_3^- belongs to Γ_{25}^-; the matrix elements with ϵ_1^-, ϵ_2^- vanish. We have the result

$$M=H_1+H_2. \tag{57}$$

In the sum N all representations appear which satisfy the selection rule (49). The contribution from Γ_2^- is simply F, as

$$\langle 1+|p_x|\beta^-\rangle=\langle 2+|p_y|\beta^-\rangle, \tag{58}$$

by reflection in the (110) plane. The contribution from Γ_{12}^- is $-G$, using Eqs. (52) and (53). The contribution from Γ_{15}^- is H_1, by reflection in the (110) plane. The contribution from Γ_{25}^- is $-H_2$, by reflection. Thus,

$$N=F-G+H_1-H_2. \tag{59}$$

It may be possible to neglect H_2 in silicon and germanium because of remoteness from the valence band.

We must now include the effect of the spin-orbit interaction, which splits the valence band edge into two levels, the upper level being fourfold degenerate ($p_{\frac{3}{2}}$) and the lower level being twofold degenerate ($p_{\frac{1}{2}}$). Our original band had a total degeneracy of $3\times 2=6$, the factor two arising from the two possible orientations of the electron spin. The diamond structure has a center of inversion; it may be shown that each band is doubly degenerate; that is, for a given energy and given k there will be two states. In our original work we incorporated the spin-orbit interaction in the problem using the results of Elliott.[36] We believe now, however, that the results will be more accessible to experimentalists and more closely related to the band energy calculations of Herman and others if presented in terms of a transformation from the $\epsilon_i m_s$ representation to the Jm_J representation.[37]

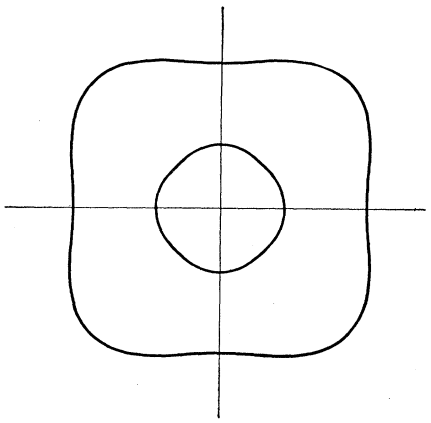

FIG. 8. Figures of constant energy in the (100) plane of k-space for the two fluted energy surfaces which are degenerate at the valence band edge; constants as for germanium.

We note first that to a good approximation we need only be concerned with the transformation of the initial unperturbed states ϵ_i^+ belonging to the representation Γ_{25}^+. A sum of the form

$$\sum_{\alpha j}\langle r+|\mathcal{H}'|\alpha j\rangle\langle\alpha j|\mathcal{H}'|s+\rangle,$$

as in Eq. (46), is invariant under a unitary transformation of the states $|\alpha j\rangle$. If we may neglect the changes in the energy denominators $E_0-E_{l\alpha}$ caused by possible spin-orbit splitting of the states $|\alpha j\rangle$, it follows that the values of the matrix elements $\langle r|\mathcal{H}'|s\rangle$ as in Eq. (43) are not altered by a transformation of the states $|\alpha j\rangle$ to diagonalize the spin-orbit interaction. We may restrict ourselves to spin-orbit effects on the initial states ϵ_i^+.

If we represent the 3×3 matrix in Eq. (46) by Y, the corresponding 6×6 matrix in the $\epsilon_i^+ m_s$ representation is, symbolically,

$$\begin{pmatrix} Y & 0 \\ 0 & Y \end{pmatrix}. \tag{60}$$

We wish to add to the perturbation the spin-orbit interaction,

$$\mathcal{H}_{so}=\frac{\hbar}{4m^2c^2}[\nabla V\times\mathbf{p}]\cdot\boldsymbol{\sigma}, \tag{61}$$

and then to diagonalize the energy matrix with respect to the spin-orbit perturbation; the Jm_J representation is diagonal in the spin-orbit interaction.

The transformed secular equation is, in terms of the

[36] R. J. Elliott, Phys. Rev. **96**, 266 (1954).

[37] This type of approach was carried out first by E. N. Adams II (unpublished).

matrix elements H_{ij} defined by Eq. (43),

$$\begin{vmatrix}
\frac{H_{11}+H_{22}}{2}-\lambda & -\frac{H_{13}-iH_{23}}{\sqrt{3}} & -\frac{H_{11}-H_{22}-2iH_{12}}{2\sqrt{3}} & 0 & -\frac{H_{13}-iH_{23}}{\sqrt{6}} & -\frac{H_{11}-H_{22}-2iH_{12}}{\sqrt{6}} \\
-\frac{H_{13}+iH_{23}}{\sqrt{3}} & \frac{4H_{33}+H_{11}+H_{22}}{6}-\lambda & 0 & -\frac{H_{11}-H_{22}-2iH_{12}}{2\sqrt{3}} & -\frac{H_{11}+H_{22}-2H_{33}}{3\sqrt{2}} & \frac{H_{13}-iH_{23}}{\sqrt{2}} \\
-\frac{H_{11}-H_{22}+2iH_{12}}{2\sqrt{3}} & 0 & \frac{4H_{33}+H_{11}+H_{22}}{6}-\lambda & \frac{H_{13}-iH_{23}}{\sqrt{3}} & \frac{H_{13}+iH_{23}}{\sqrt{2}} & \frac{H_{11}+H_{22}-2H_{33}}{3\sqrt{2}} \\
0 & -\frac{H_{11}-H_{22}+2iH_{12}}{2\sqrt{3}} & \frac{H_{13}+iH_{23}}{\sqrt{3}} & \frac{H_{11}+H_{22}}{2}-\lambda & \frac{H_{11}-H_{22}+2iH_{12}}{\sqrt{6}} & -\frac{H_{13}+iH_{23}}{\sqrt{6}} \\
-\frac{H_{13}+iH_{23}}{\sqrt{6}} & -\frac{H_{11}+H_{22}-2H_{33}}{3\sqrt{2}} & \frac{H_{13}-iH_{23}}{\sqrt{2}} & \frac{H_{11}-H_{22}-2iH_{12}}{\sqrt{6}} & \frac{H_{11}+H_{22}+H_{33}}{3}-\lambda-\Delta & 0 \\
-\frac{H_{11}-H_{22}+2iH_{12}}{\sqrt{6}} & \frac{H_{13}+iH_{23}}{\sqrt{2}} & \frac{H_{11}+H_{22}-2H_{33}}{3\sqrt{2}} & -\frac{H_{13}-iH_{23}}{\sqrt{6}} & 0 & \frac{H_{11}+H_{22}+H_{33}}{3}-\lambda-\Delta
\end{vmatrix}=0. \quad (62)$$

In Eq. (62), Δ denotes the spin-orbit splitting of the $p_{\frac{3}{2}}$, $p_{\frac{1}{2}}$ levels. As all H_{ij} are of order k^2, we may approximate the determinant by considering only the elements in the 4×4 block in the upper left corner and in the 2×2 block in the lower right corner. The elements in the two 2×4 strips neglected in this approximation affect the roots only in the order k^4/Δ. The roots of the 4×4 are

$$E(k)=Ak^2\pm[B^2k^4+C^2(k_x^2k_y^2+k_y^2k_z^2+k_z^2k_x^2)]^{\frac{1}{2}}, \quad (63)$$

where

$$\begin{aligned} A&=\tfrac{1}{3}(L+2M)+\hbar^2/2m; \\ B&=\tfrac{1}{3}(L-M); \\ C^2&=\tfrac{1}{3}[N^2-(L-M)^2]. \end{aligned} \quad (64)$$

Each root occurs twice, so that each of the two bands is double; this degeneracy results from the inversion symmetry element of the diamond structure, and is presumably lifted in the zinc blende structure, which includes InSb and other 3–5 semiconductors. The energy surfaces described by Eq. (63) are nonspherical for $C\neq0$, and are known as fluted or warped surfaces. In Fig. 8 we have plotted in the (100) plane in k-space lines of constant energy for the surfaces in germanium.

The roots of the 2×2 block in Eq. (62) are

$$E(k)=-\Delta+Ak^2, \quad (65)$$

where the constant A is identical with that in Eq. (64) if the spin-orbit splitting Δ may be neglected in comparison with the relevant energy denominators, which are of the order of the forbidden energy gap. This approximation is likely to be satisfactory in silicon, where Δ may be of the order of 0.04 ev, but in germanium Δ is thought to be about 0.3 ev, according to the analysis of Kahn[38] of infrared absorption results in p-Ge. It should be noted that if Δ in silicon is indeed of the order of 0.04 ev, our quadratic expression (63) for the band edge may not be an adequate approximation to describe carriers in thermal equilibrium at room temperature.

[38] A. Kahn, Phys. Rev. **97**, 1647 (1955); thesis, Berkeley, 1954 (unpublished).

The energies near $\mathbf{k}=0$ of other states not split by the spin-orbit interaction are

$$E(\Gamma_1^{\pm})=\frac{\hbar^2k^2}{2m}\left(1+\frac{2}{m}\sum_{\Gamma_{15}^{\mp}}\frac{|\langle\alpha^{\pm}|p_x|\delta_{1l}^{\mp}\rangle|^2}{E_0-E_l}\right); \quad (66)$$

$$E(\Gamma_2^{\pm})=\frac{\hbar^2k^2}{2m}\left(1+\frac{2}{m}\sum_{\Gamma_{25}^{\mp}}\frac{|\langle\beta^{\pm}|p_x|\epsilon_{1l}^{\mp}\rangle|^2}{E_0-E_l}\right); \quad (67)$$

$$E(\Gamma_{12}^{\pm})=k^2(\hbar^2/2m+J+K)\pm(J-K)[k^4-3(k_x^2k_y^2+k_y^2k_z^2+k_z^2k_x^2)]^{\frac{1}{2}}; \quad (68)$$

where

$$\begin{aligned} J&=\frac{\hbar^2}{m^2}\sum_{\Gamma_{15}^{\mp}}\frac{|\langle\gamma_1^{\pm}|p_x|\delta_{1l}^{\mp}\rangle|^2}{E_0-E_l}, \\ K&=\frac{\hbar^2}{m^2}\sum_{\Gamma_{25}^{\mp}}\frac{|\langle\gamma_1^{\pm}|p_x|\epsilon_{1l}^{\mp}\rangle|^2}{E_0-E_l}. \end{aligned} \quad (69)$$

In germanium, where the Γ_2^- state is believed to be the lowest conduction band state, the energy near $\mathbf{k}=0$ is

$$E(\Gamma_2^-)\cong k^2[(\hbar^2/2m)+|F|]. \quad (71)$$

Using the experimental values of the constants [see Eq. (81)], this gives $m^*/m\cong0.034$. Estimates of the effective masses for other higher conduction states at $k=0$ seem unjustified, as the perturbations on these states will include important terms other than the Γ_{25}^+ valence state.

The fluted or warped quality of the energy surfaces near the valence band edge has a complicated effect on the cyclotron resonance frequency. There is no longer, as with the ellipsoidal surfaces, a single cyclotron frequency for a given orientation of the static magnetic field relative to the axes of the energy surface, but there is now a distribution of resonance frequencies. We give a discussion of the distribution on the assumption that the quantum numbers involved are sufficiently high so that a semiclassical treatment is valid; the quantum theory has been discussed by Luttinger and Kohn,[39] and they find departures from the classical theory at low quantum numbers.

[39] J. M. Luttinger, and W. Kohn Phys. Rev. **97**, 869 (1955).

We suppose that we have a general effective mass Hamiltonian $\mathcal{H}(\mathbf{P})$, where $\mathbf{P}=\hbar\mathbf{k}$. The magnetic field in a classical limit does not change the energy of a particle moving on the energy surface, nor does it change the projection P_H of the $\mathbf{P}$ vector along the magnetic field direction. The motion of the particle is confined to the region in dP_H at P_H and with energy in dE at E; the region has been called a tube by Shockley.[40] The effective mass for cyclotron resonance on any closed tube has been given by Shockley. From Eq. (33) we have $cdP=ev_\alpha H dt$, where v_α is the scalar magnitude of the projection of the group velocity $\mathbf{v}$ on a plane perpendicular to the magnetic field. Then

$$\oint \frac{cdP}{eHv_\alpha}=\frac{2\pi}{\omega_c}, \tag{72}$$

where ω_c is the fundamental angular frequency of the motion. Higher harmonics are present generally, but are not derived in our present analyses. We define a tube mass m^* such that $\omega_c=eH/m^*c$; thus,

$$m^*=\oint dP/(2\pi v_\alpha). \tag{73}$$

It is always possible, of course, to work directly with the equations of motion, but we have found the integral expression for the mass to be quite convenient. We should emphasize that this equation has been derived in what is essentially a classical limit; the fact that the experimental results appear to be more or less independent of the rf power over a wide range gives us some confidence in the equation; variations in temperature by a factor of two also do not have obvious effects on the positions of the resonance lines.

The cyclotron tubes with $k_H\approx 0$ have the important property that their effective mass remains unchanged as the particle is accelerated and the orbit opens out under the influence of the rf electric field. It is likely, particularly in conditions of high rf power, that the orbits of small k_H have an important effect on the resonance line arising from a fluted energy surface. In other words, the distribution function may be changed by the rf field so as to emphasize small k_H.

We introduce for $\mathbf{k}$ a cylindrical coordinate system, k_H, ρ, ϕ, with k_H parallel to the applied magnetic field; ρ is the radial coordinate in the plane in k-space perpendicular to k_H. By an elementary transformation of Eq. (73), we have

$$m^*=\frac{\hbar^2}{2\pi}\oint \frac{\rho d\phi}{(\partial E/\partial\rho)}. \tag{74}$$

The application of this result to the valence band edge of silicon and germanium is generally formidable. The result is fairly tractable for H parallel to a (110) plane and for the equatorial tubes $k_H=0$. We have, under these restrictions,

$$m^*=(\hbar^2/\pi)\int_0^{\pi/2}\frac{d\phi}{A\pm\{B^2+\frac{1}{4}C^2[1+g(\phi)]\}^{\frac{1}{2}}}, \tag{75}$$

where A, B, C are defined by Eq. (63), and

$$g(\phi)=-(3\cos^2\theta-1)[(\cos^2\theta-3)\cos^4\phi+2\cos^2\phi], \tag{76}$$

with θ the angle the magnetic field makes with the [100] direction.

An expansion in power of $g(\phi)$ gives

$$m^*=\frac{\hbar^2}{2}\frac{1}{A\pm[B^2+(C/2)^2]^{\frac{1}{2}}} \times\left\{1\pm\frac{C^2(1-3\cos^2\theta)^2}{64[B^2+(C/2)^2]^{\frac{1}{2}}\{A\pm[B^2+(C/2)^2]^{\frac{1}{2}}\}}+\cdots\right\}. \tag{77}$$

This result is exact for the [111] direction; in other directions the contribution of the next term in the expansion is not greater than about 1 percent in silicon and germanium.

We have evaluated the constants A, B, C by making a fit of m^* as given by Eq. (77) to the experimental data on the two cyclotron resonance lines associated with the valence band. This procedure is justified if the position of the center of the resonance line is given approximately by the carriers which have $k_H\approx 0$. There are two arguments which support this procedure; the first argument given above is that the orbits near $k_H=0$ maintain their frequency constant as they are accelerated outward; the second argument is that m^* is fairly independent of k_H, except for high k_H, which are discriminated against by a geometrical factor in the density of states. In Fig. 9 we give the results of calculations of m^* *vs* k_H for germanium in the [100] and [111] directions. The contributions of high k_H are principally in one wing of the resonance line.

In Fig. 10 we give a plot of the experimental points for holes in germanium at 4°K as a function of the angle between the direction of the static magnetic field in a (110) plane and a [001] direction lying in the plane. The constants A, B, C in the expression (63),

$$E(k)=Ak^2\pm[B^2k^4+C^2(k_x^2k_y^2+k_y^2k_z^2+k_zk_x^2)]^{\frac{1}{2}}, \tag{78}$$

are determined from the experimental data, using Eq (77). The theoretical curve in the figure is calculated using the values

$$\begin{aligned} A&=-(13.0\pm0.2)(\hbar^2/2m);\\ |B|&=(8.9\pm0.1)(\hbar^2/2m);\\ |C|&=(10.3\pm0.2)(\hbar^2/2m). \end{aligned} \tag{79}$$

These values represent our best fit for germanium. Dexter, Zeiger, and Lax[41] have reported $A=-13.6(\hbar^2/$

[40] W. Shockley, Phys. Rev. **79**, 191 (1950).

[41] Dexter, Zeiger, and Lax, Phys. Rev. **95**, 557 (1954).

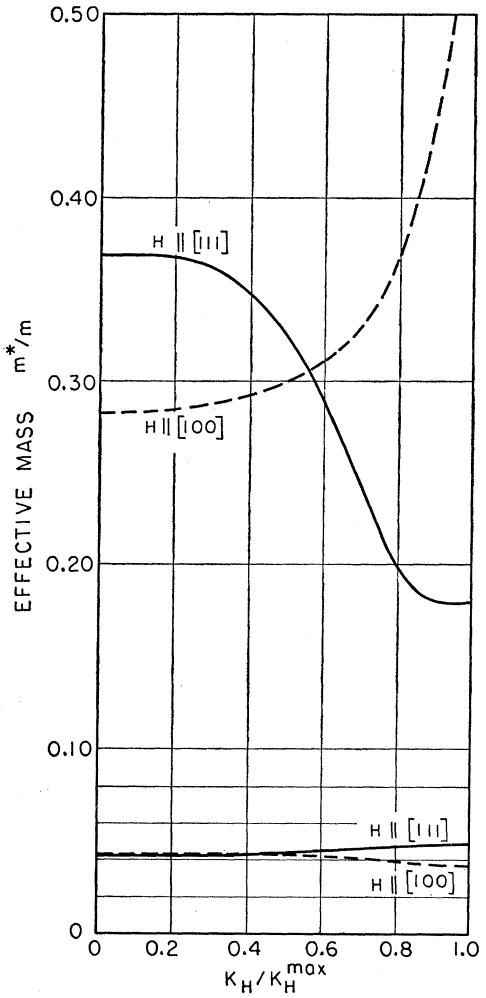

FIG. 9. Calculated values of m^* *vs* the component k_H of the **k**-vector along the direction of the static magnetic field, for the [100] and [111] directions in germanium.

$2m$); $|B|=9.1(\hbar^2/2m)$; $|C|=11.2(\hbar^2/2m)$. Our error estimates in (79) represent the scatter of the experimental points about the theoretical curve; because of the use of the assumption $k_H\approx 0$, the correct constants may possibly lie outside of the indicated limits. An attempt by us to take into account the distribution of k_H gives the following approximate constants: $A=-(13.2\pm 0.1)(\hbar^2/2m)$; $|B|=(8.9\pm 0.05)(\hbar^2/2m)$; $|C|=(10.6\pm 0.2)(\hbar^2/2m)$.

In Fig. 11 we give a plot of the experimental points for holes in silicon at 4°K. The theoretical curve is calculated using the values

$$\begin{aligned} &A=-(4.1\pm 0.2)(\hbar^2/2m);\\ &|B|=(1.6\pm 0.2)(\hbar^2/2m);\\ &|C|=(3.3\pm 0.5)(\hbar^2/2m). \end{aligned} \tag{80}$$

Dexter and Lax[42] have reported $A=-4.0(\hbar^2/2m)$; $|B|=1.3(\hbar^2/2m)$; $|C|=3.6(\hbar^2/2m)$. An attempt by us to take into account the distribution of k_H gives the following approximate constants: $A=-(4.0\pm 0.2)(\hbar^2/2m)$; $|B|=(1.1\pm 0.5)(\hbar^2/2m)$; $|C|=(4.0\pm 0.5)(\hbar^2/2m)$.

Using relations (54), (57), (59), (64), together with the experimental results from (79) and (80), the values of the sums over matrix elements in germanium are

$$\begin{aligned} &L=-31.8(\hbar^2/2m); \quad F=-28.6(\hbar^2/2m);\\ &M=-5.1(\hbar^2/2m); \quad G=-1.6(\hbar^2/2m);\\ &N=-32.1(\hbar^2/2m); \quad H_1=-5.1(\hbar^2/2m);\\ &\qquad\qquad\qquad H_2=0; \end{aligned} \tag{81}$$

and, in silicon,

$$\begin{aligned} &L=-1.9(\hbar^2/2m); \quad F=-1.2(\hbar^2/2m);\\ &M=-6.7(\hbar^2/2m); \quad G=-0.4(\hbar^2/2m);\\ &N=-7.5(\hbar^2/2m); \quad H_1=-6.7(\hbar^2/2m);\\ &\qquad\qquad\qquad H_2=0. \end{aligned} \tag{82}$$

If we neglect the spin-orbit splitting of the valence band edge in comparison with the other energy denominators, the effective mass of the $p_{\frac{1}{2}}$-band should be, from Eq. (65), $m^*\cong 0.08m$ in germanium and $m^*=0.25m$ in silicon. The value for germanium is in satisfactory agreement with Kahn's interpretation of the infrared absorption spectrum of p-Ge. These constants are not uniquely determined from A, B, and C, because Eqs. (64) are not linear. The constant H_2 was assumed zero due to the presumed remoteness of the Γ_{25}^- state from the valence band. The choice of constants above was made because the sums over matrix elements are all negative, as expected if the conduction

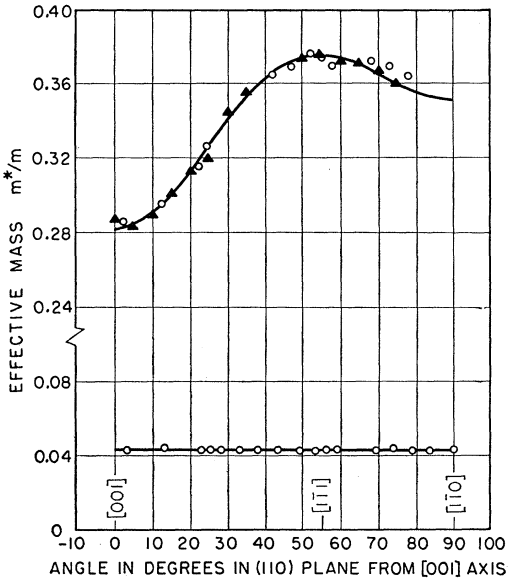

FIG. 10. Effective mass of holes in germanium at 4°K for magnetic field directions in a (110) plane; the theoretical curves are obtained from Eq. (77), using the constants in Eq. (79).

[42] R. N. Dexter and B. Lax, Phys. Rev. **96**, 223 (1954).

states furnish the main perturbation. In silicon there is another set of solutions in which all sums over matrix elements are negative, but the order of magnitude of the constants seemed unlikely. The constants above are in line with the model proposed by Herman.[43] We note that perturbations with Γ_2^- are dominant in germanium, and with Γ_{15}^- are dominant in silicon.

We have analyzed, using Eq. (8), the line widths observed at 4°K in the specimens which gave the sharpest lines. The relaxation times for electrons were approximately isotropic, with $\tau(\text{Ge})\cong 6\times 10^{-11}$ sec and $\tau(\text{Si})\cong 7\times 10^{-11}$ sec. The effective relaxation times for the light mass hole resonances were $\tau(\text{Ge})\cong 7\times 10^{-11}$ and $\tau(\text{Si})\cong 7\times 10^{-11}$ sec; for the heavy mass hole resonances, $\tau(\text{Ge})\gtrsim 5\times 10^{-11}$ sec and $\tau(\text{Si})\gtrsim 6\times 10^{-11}$ sec. These data were taken with optical excitation of carriers. The lines did not appear to sharpen appreciably on pumping to 2°K, but the specimens may possibly have been at a higher temperature. At rf power levels below the ionization limit it did not appear that the widths were dependent on the rf power levels in the range covered. The line shapes of the electron resonances appeared to be approximately Gaussian, while the elementary theory predicts a Lorentzian shape.

Several remarks can be made about the relative intensity of the light and heavy mass hole resonance lines. At the resonance maximum the energy losses are proportional, according to Eq. (15), to the static conductivity $\sigma_0=Ne^2\tau/m^*$. Therefore,

$$\frac{I(l)}{I(h)}=\frac{N_l}{N_h}\frac{m_h}{m_l}\frac{\tau_l}{\tau_h}. \tag{83}$$

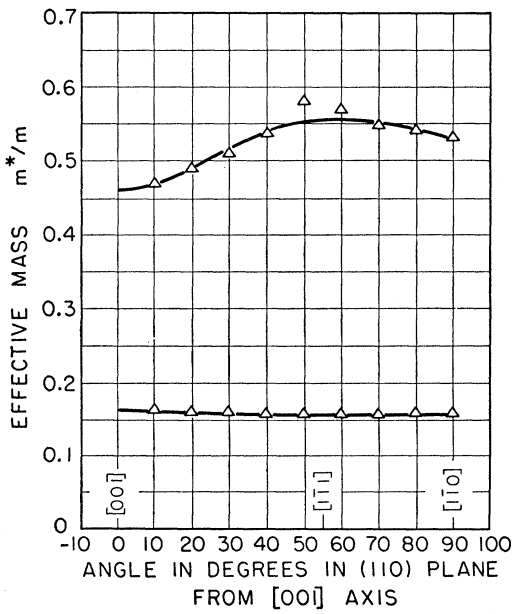

FIG. 11. Effective mass of holes in silicon at 4°K for magnetic field directions in a (110) plane; the theoretical curves are obtained from Eq. (77), using the constants in Eq. (80).

[43] F. Herman, Phys. Rev. **95**, 847 (1954).

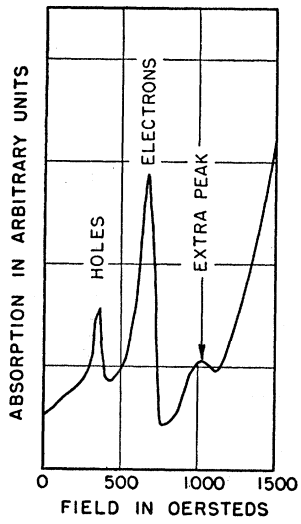

FIG. 12. Possible extra line, as indicated in germanium at 55° from a [001] direction in a (110) plane.

If the population ratio N_l/N_h of the two bands is determined by considerations of thermal equilibrium, we have

$$N_l/N_h=(m_l/m_h)^{\frac{3}{2}}, \tag{84}$$

as the volume in phase space corresponding to an energy range ΔE is proportional to $(m^*)^{\frac{3}{2}}$. Thus,

$$I(l)/I(h)=(m_l/m_h)^{\frac{1}{2}}(\tau_l/\tau_h). \tag{85}$$

In silicon and germanium it appears that $\tau_l\cong\tau_h$, so we would expect, roughly,

$$\text{Ge: } I(l)/I(h)\cong\tfrac{1}{8};\quad \text{Si: } I(l)/I(h)\cong\tfrac{1}{2}; \tag{86}$$

as the average mass ratio is about $\frac{1}{8}$ for germanium and $\frac{1}{3}$ for silicon.

The integrated intensity will be proportional to the product of the peak intensity and the line width $\Delta\omega_c=1/\tau=(e/m^*c)\Delta H$, so that the integrated intensity ratio is

$$g(l)/g(h)=(m_l/m_h)^{\frac{3}{2}}. \tag{87}$$

We therefore expect

$$\text{Ge: } g(l)/g(h)\cong 1/20;\quad \text{Si: } g(l)/g(h)\cong 1/5. \tag{88}$$

The experimental ratios are consistent with these estimates.

6. FURTHER REMARKS

Kip[44] at the Amsterdam Conference reported the tentative observation in germanium of several extra lines, that is, lines which cannot be assigned to the hole or electron band edge energy surfaces. The observational situation on the extra lines is rather unsatisfactory at the moment, as one of the lines (the one shown in Fig. 12) is feeble and does not often appear. The second extra line (not shown) is erratic in appearance, and when it does appear it is rather too strong to be creditable; we are inclined to believe that at least in our own work the appearance of the second

[44] A. F. Kip, Physica **20**, 813 (1954).

line may often be accounted for by a slight misorientation of the specimen, as a 5° misorientation can remove the degeneracy of one of the electron resonance lines in the (110) plane by a splitting of as much as 200 to 300 oersteds for some directions. There are several mechanisms which one might invoke for the production of extra lines, including (a) the possibility of resonance on excited bands or near higher local minima on the usual band; (b) partial breakdown of the selection rule $\Delta n=\pm 1$ on the fluted surfaces, as suggested privately by Dexter, Lax, and Zeiger; (c) nonclassical effects at low temperatures, as hinted at by Kohn and Luttinger[45]; (d) distortion of the form of the energy surfaces in the valence band at small k as a result of the Zeeman splitting of the band edge states; and (e) if the plot of m^* *vs* k_H should be horizontal at several separated k_H values, extra lines should appear.

We have recently observed cyclotron resonance of electrons and holes in InSb, and we have a preliminary indication of cyclotron resonance in InAs. Details of this work will be published separately.

[45] W. Kohn and J. M. Luttinger, Phys. Rev. **96**, 529 (1954).

ACKNOWLEDGMENTS

We have had a great deal of valuable assistance from many persons and organizations in this work. Financial support is gratefully acknowledged from the U. S. Office of Naval Research, the U. S. Signal Corps, the National Science Foundation, and the Pittsburgh Plate Glass Foundation. We are especially indebted for the supply of semiconductor crystals to the Bell Telephone Laboratories, to Sylvania Electric Products, Inc., and to the Westinghouse Research Laboratories. Liquid helium was kindly furnished by Professor W. F. Giauque and Dr. D. N. Lyons. The crystals were oriented by Prof. J. Washburn. J. Ubbink, G. Feher, and Glen Wagoner assisted with the measurements. We wish to express our thanks to the Lincoln Laboratory group associated with Dr. B. Lax for their friendly exchange of information on their work. We have profited from correspondence and conversations with E. N. Adams II, P. Aigrain, W. B. Brattain, E. Burstein, E. Conwell, R. E. Davis, R. J. Elliott, H. Y. Fan, R. Fletcher, M. J. E. Golay, F. Herman, C. Herring, R. Longini, F. J. Morin, H. M. O'Bryan, F. Seitz, W. Shockley, and A. F. Siefert.

PHYSICAL REVIEW VOLUME 98, NUMBER 2 APRIL 15, 1955

Measurement of Shot Noise in CdS Crystals

C. I. SHULMAN
RCA Laboratories, Princeton, New Jersey
(Received September 21, 1954)

The noise power spectrum associated with photoconduction current in CdS crystals with indium electrodes is found to flatten off at low frequencies at a value that corresponds closely to the noise inherent in the photon absorption process itself plus that associated with the random nature of the carrier recombination process. It is found that the noise power is not a unique function of the photoconduction current, but varies as the square of the applied voltage, and linearly with light intensity, as suggested by a simple model not unlike that of the photomultiplier.

MEASUREMENTS of noise associated with the passage of current through semiconducting materials have led to a variety of theories,[1–4] most of which center about boundary layer phenomena. The essential observations that these models seek to derive are (1), the large excess of noise relative to thermal and (2) a $1/f$ spectrum down to extremely low frequencies. Most of the models are complicated and have the flexibility to account for a wide range of spectra and often do, in fact, give a fairly good fit with observation. There are simple models[5,6] involving processes within the body of the semiconductor itself which yield spectra that flatten off at low frequencies and give noise levels much lower than those reported by most observers. These models are rather straightforward and simple, and represent a possible reference for the study of inner processes in semiconductors, for if the strong fluctuations associated with boundary layer phenomena could be eliminated, one would gain a useful tool for the study of current flow in solids. It is the purpose of this note to describe work wherein it was found possible to make noiseless ohmic contact to CdS crystals such that the noise associated with the passage of current through the crystal could be interpreted in terms of processes within the CdS crystal itself.[7]

In the study of the electrical properties of crystals there is always the important general question of separating out the effects of contact electrodes and their interaction with the material under study. Such interactions often cause nonlinear volt-ampere characteristics and nonlinear potential distributions within the body of crystals. The use of gallium[8] or indium as

[1] W. Schottky, Phys. Rev. **28**, 74 (1926).
[2] G. G. McFarlane, Proc. Phys. Soc. (London) **59**, 366 (1947).
[3] A. Van D. Ziel, Physica **16**, 359 (1950).
[4] W. M. Buttler, Ann. Physik. **11**, 362 (1953).
[5] B. Davydov and B. Gurevich, J. Phys. (U.S.S.R.) **7**, 138 (1943).
[6] J. H. Gisolf, Physica **15**, 825 (1949).
[7] Shulman, Smith, and Rose, Phys. Rev. **92**, 857(A) (1953).
[8] R. W. Smith, Phys. Rev. **92**, 857 (1953).